Reliability of Tantalum Polymer Capacitors

Jonathan L. Paulsen, Erik K. Reed, Jeffrey N. Kelly
KEMET Electronics Corporation
PO Box 5928
Greenville, SC 29606
Tel:864-963-6300
Fax: 864-228-4333
jonathanpaulsen@kemet.com, erikreed@kemet.com, jeffkelly@kemet.com

Abstract

The demand for Low-ESR tantalum capacitors has popularized the use of high conductivity conductive polymer counter electrode designs over more established manganese dioxide (MnO_2) tantalums. While the reliability of MnO_2 tantalums has been well studied, the expected performance of conductive polymer tantalums is less understood. To characterize the reliability of polymer tantalums, accelerated lifetesting utilizing high electric field stress and temperature is performed on multiple test samples. The time-to-failure data is fit to a failure model and the model is then used to predict device reliability under less strenuous conditions. Considering all the data, median life for the test sample at maximum rated conditions was found to exceed 300 years.

Introduction

Tantalum chip capacitors have been successfully manufactured with manganese dioxide (MnO_2) solid electrolyte for decades and much has been learned and published regarding their reliability in a wide range of applications. The push for lower equivalent series resistance (ESR) in tantalum chip capacitors has lead to the use of conductive polymers in place of MnO_2. Because the conductive polymers employed are significantly more electrically conductive than MnO_2, capacitors with equivalent series resistance below 10mΩ are possible.

Unfortunately, because of their recent introduction, not much is known about the inherent reliability of tantalum polymer capacitors. Moreover, the applications in which low-ESR tantalum polymer capacitors are used are among the most demanding from a reliability perspective. So, just how reliable are tantalum polymer capacitors?

Manufacturers' in-house reliability test results and early field experiences with polymer capacitors are very good, in most cases superior to similarly valued capacitors manufactured with MnO_2. The purpose of this paper is to present reliability data from tantalum polymer capacitors. Similarities in reliability to MnO_2 are expected because of the dominant influence of the Ta_2O_5 dielectric which is largely unaffected by the choice of solid electrolyte. But differences do exist. By developing a framework for accelerated lifetest analysis, this work aims to highlight any differences from traditional tantalum capacitors that may affect reliability.

System Description

The block diagram for the time-to-failure system used for these experiments is shown in fig. 1.

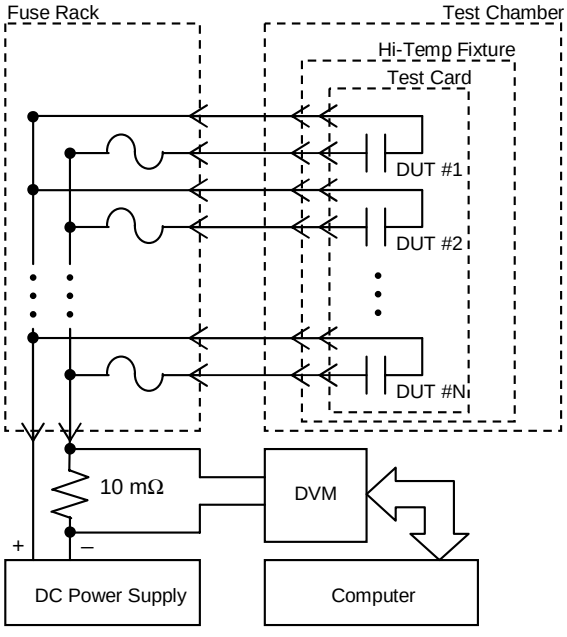

Fig. 1. Time-To-Failure System Block Diagram.

This test system comprises seven basic elements. The test parts are mounted onto test cards which are placed into connectors mounted to a fixture within the test chamber. The test card fixture has multiple 22 position connectors rated for use at high temperatures (up to 200°C). The number of connectors within the system depends upon the size of the test chamber and the desired sample size for the test. Fixtures used for these experiments range from 5 to 12 connectors. The test chamber itself is a general purpose environmental chamber capable of operation at temperatures from -55°C to 250°C. Wires soldered to the high-temp connectors are routed through a port in the test chamber to a rack outside the test environment which holds 1 amp fuses connected in series with each part under test. Each test part circuit has a resistance below 600mΩ. The entire fuse rack is wired to the output of a DC power supply. A 10mΩ current measurement resistor is placed in series with the negative power supply lead. A high speed digital voltmeter is connected across the 10mΩ resistor to measure any voltage caused by current passing through the test system. The voltmeter communicates with a computer running software which detects failures as they occur and records their time relative to the start of the test.

System Operation

All devices arrived for testing sealed in an airtight bag and packed with desiccant. Once sample mounting on test boards was complete, unused parts were placed back in the sealed bag with desiccant to minimize moisture absorption during the experiment. Following mounting, all test samples were loaded into the test fixture and the temperature in the chamber was bought up to test conditions (85° - 165°C). After temperature stabilization, the output of the DC power supply was switched on and the digital voltmeter (DVM) began monitoring the voltage across the current measurement resistor several thousand times per second. Once the initial charging transient had faded, only a small amount of leakage current would flow through the test circuit (typically 100's of microamps, depending on sample size). As failures occurred, the fuses blew open and current spikes were detected by the DVM. The magnitude of these failure surges was far greater than the background leakage current. Fig. 2 shows a plot of typical current history for one part during testing. Because of low sampling rate, the true peak current of several amperes does not appear in the figure. Current spikes from 3-4 amps for 120 milliseconds were common failure indicators.

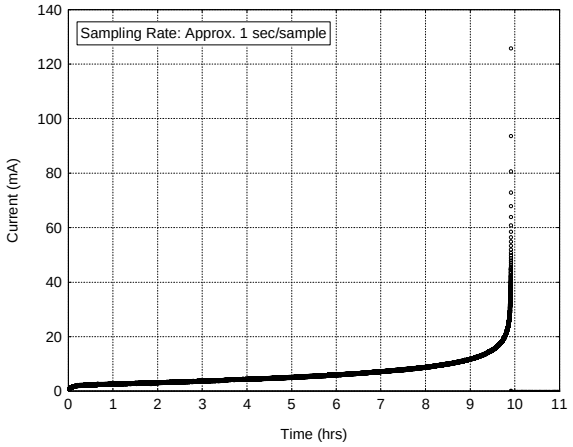

Fig. 2. Failure Current versus Time.

When inserted into the oven fixture, all test cards were arranged vertically, with 1" spacing between adjacent cards. All boards were arranged in parallel and then positioned with respect to airflow within the chamber for minimal temperature variation across the length of the fixture. Results of this experiment indicate the temperature of the test samples does have a significant impact on their time-to-failure in accelerated testing. Therefore, a temperature variation of less than 3°C across the entire fixture was verified prior to testing.

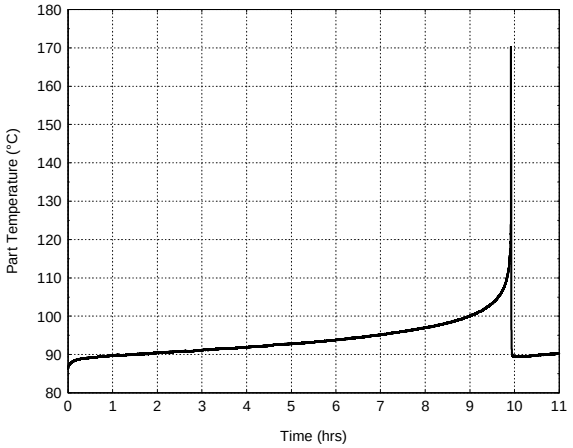

Fig. 3. Device-under-Test Temperature During Failure.

As shown in fig. 2, current through the test samples was observed to rise for several hours prior to failure. During this period, component self-heating due to high leakage current contributed to elevated temperatures within the parts themselves. Fig. 3

shows a plot of device temperature during its failure period.

Airflow in the chamber and self-heating introduce two complicating factors into the data analysis of this experiment. First, self-heating clearly elevates the part temperature above the intended test temperature. Although this effect certainly occurs in conventional device applications during failure, it makes the process of predicting performance at different conditions more difficult. Ultimately, this self heating causes an interaction between temperature and voltage that is shown to affect test results. Secondly, the carefully controlled airflow in the test chamber may also contribute to experimental error. An argument could be made that most tantalum capacitors do not benefit from such efficient air cooling during normal use. While this airflow helps maintain the proper temperature during the initial phases of the accelerated testing, it may serve to cool the part during its self-heating phase and artificially prolong its life.

Occasionally, a test part would begin to pull excessive current during its failure phase, but internal heating would quickly cause the conductive materials within the part to change and detach from the outer contacts before the series fuse could blow. This "fail open" condition would produce visible damage to the fuse wire and indicate a failure on the tester. Fig. 4 displays a fuse damaged in this way as well as fuse appearance during other phases of testing. Despite fuse survival in these cases, the parts were still regarded as failures due to their initial internal shorting and resulting open condition.

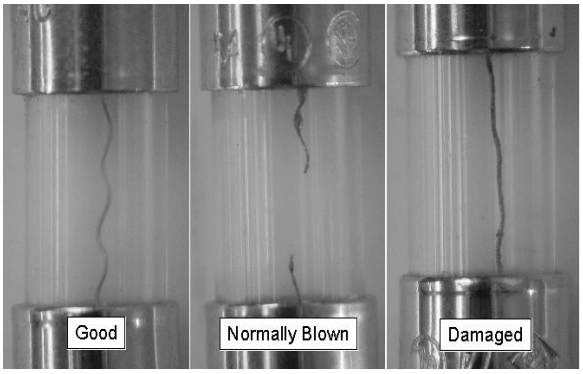

Fig. 4. Fuse Appearance for Normal, Blown and Damaged Conditions.

Failure Modeling

Accelerated lifetest analysis of tantalum capacitors with MnO_2 counter electrodes has traditionally been accomplished using Weibull failure rate grading as outlined in military performance specification 39003J. The capacitors were exposed to a multiple of rated voltage, typically 1.1 to 1.5 times rated voltage, and tested at 85°C until a sufficient number of failures were observed for calculations. The acceleration of time-to-failure for each test batch was obtained using equation (1). This equation, devised by the Crane Laboratory of the Naval Weapons Support Center in the late 1970's, utilizes values derived by combining the results of accelerated lifetest results from many tantalum capacitor samples from multiple manufacturers.

$$A = 7.03412025 \times 10^{-9} e^{18.77249321 \times \frac{V_a}{V_r}} \quad (1)$$

Experimental data collected over the years has raised questions regarding the validity of this formula. Subsequent investigations have demonstrated that the acceleration factor can vary widely from batch to batch among similar parts; even from the same supplier. The attempt to combine the results of many batches from many manufacturers resulted in an equation that did not apply particularly well to any traditional tantalum part type with the amount of precision suggested in the formula.

Even though the validity of the acceleration formula was suspect, observed failure rates in MnO_2 tantalums were typically low enough to accommodate a large margin of error without concern.

MnO_2 counter electrode tantalums generally demonstrate declining failure rates in Weibull grading tests. In many of these cases, however, a distinct wearout phase was never observed, perhaps because the tests were not long enough at the given conditions. In the absence of observed wearout, and in the presence of declining failure rate, characteristic lifetimes were projected to be incredibly long. But it is suspected that at some point wearout would be observed. In this experiment, tantalum capacitors made with conductive polymer counter electrodes were lifetested with enough acceleration to actually reach wearout within a reasonable timeframe. Observing all the failure modes in these devices, including wearout, suggested the use of a different, more accurate acceleration model.

An established formula for modeling acceleration in time for capacitor lifetest failures as a function of voltage and temperature is the equation proposed by Prokopowicz and Vaskas, shown in equation (2).[1]

$$A = \frac{t_1}{t_2} = \left(\frac{V_2}{V_1}\right)^{\eta} e^{\left[\frac{Ea}{k}\left(\frac{1}{T_1}-\frac{1}{T_2}\right)\right]} \qquad (2)$$

This model has been used successfully for years with multilayer ceramic capacitors to interpret results from accelerated testing and to predict typical capacitor lifetimes.[2] The formula relates the ratio of different times-to-failure to the applied voltage and ambient temperature of two different test conditions. The formula can be broken into two parts. The power law portion of equation (2) quantifies time-to-failure acceleration due to the ratio of two voltages. The voltage stress exponent in the power law equation, *n*, must be experimentally derived. The second half of equation (2) accounts for time-to-failure acceleration due to changes in absolute temperature. This portion of the relation is modeled by an Arrhenius equation. The activation energy in the Arrhenius equation, *Ea*, must also be derived experimentally before equation (2) can be used.

The constant, *k*, is Boltzmann's constant. The approximate value for *k* is shown in equation (3). Absolute temperature in Kelvins is the temperature in Celsius degrees plus 273.

$$k = 8.6\times10^{-5} eV/K \qquad (3)$$

The Prokopowicz and Vaskas equation offers several advantages over the older Weibull grading formula. While the older formula was intended only for test temperature of 85°C, equation (2) accommodates any temperature in its calculation. Also, unlike equation (1), the Prokopowicz and Vaskas model is not based on a fixed level of performance measured only at one point in time, but rather has parameters that can be adjusted to reflect evolutionary changes in capacitor design and performance. To use equation (2), the voltage stress exponent and activation energy must first be found from experiments. Although this may necessitate more work initially, it produces more accurate acceleration factors and more realistic component lifetime predictions.

The time-to-failure data produced in this experiment was plotted on lognormal graphs rather than Weibull plots. Previously, time-to-failure data for tantalum capacitors was generally fit to a Weibull distribution for analysis. For Weibull plots, the statistic $t_{63.2}$, or characteristic life, is chosen rather than the median life, t_{50}. The time-to-failure data collected in this experiment was initially fit to both Weibull and lognormal distributions. Upon review, the lognormal distribution provided superior fit to the data. As a result, the median life statistic, t_{50}, was used to calculate the voltage stress exponent as well as the activation energy for use in equation (2).

Because median life is used for the times-to-failure, t_1 and t_2, in equation (2), calculations from equation (2) produce median life predictions at other levels of temperature and voltage stress. A note of caution, the statistic t_{50} should not be confused with the statistic mean-time-to-failure (MTTF) which is more properly used to describe devices whose lifetimes have an exponential distribution and which display a constant failure rate.[3]

Analysis of Time-To-Failure Data

Figure 5 contains all the time-to-failure data collected from a batch of KEMET B-case, 100µF, 6V conductive polymer tantalum capacitors. Although the data shown in fig. 5 will be presented in smaller groups subsequently, all the data sets share certain characteristics which can be observed collectively. Each line represents a sample of parts tested at a particular voltage and temperature. The parallel nature of all the data sets and the straight lines formed by the data points suggest that all failures were due to the same failure mechanism. The onset time of this failure mechanism varied due the total stress applied to each test group.

Three failure mechanisms are of interest when lifetesting tantalum capacitors: infant mortals, freaks, and wearout failures. Infant mortals contain major construction defects and never function properly. Freak failures have minor construction defects that will eventually cause failure, but perhaps years after initial usage. Wearout failures, the focus of this experiment, only occur after the dielectric within the capacitor changes as a result of applied electric field stress and temperature. All three mechanisms can be observed in lognormal plots of the time-to-failure data produced in accelerated testing. Once graphed, each failure mechanism will appear as a subpopulation requiring a different fit line.

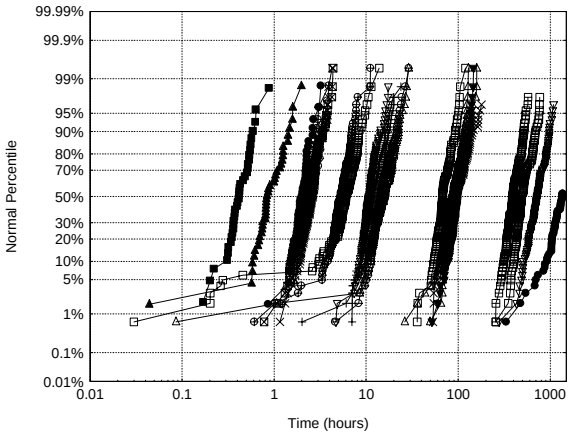

Fig. 5. Lognormal Plot of Failure Percentile versus Time-To-Failure for KEMET Polymer Tantalum Capacitors.

Referring to the data presented in Fig. 5, a few of the datasets appear to contain freak failures, their presence causing a slight curve at the bottom of the distribution. Causes for these failures are important for overall reliability assessments, but have been ignored here to focus attention on the wearout failure mode.

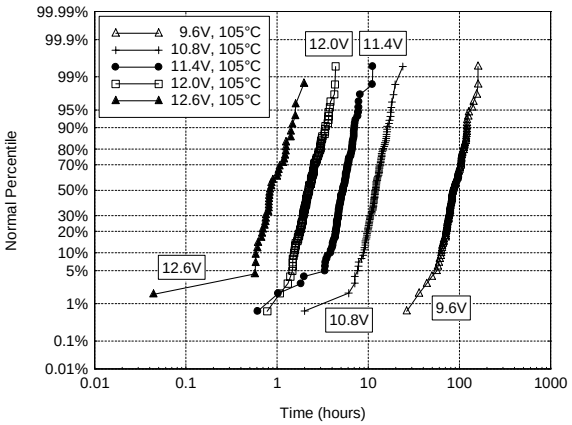

Fig. 6. Lognormal Plot of Failure Percentile versus Time-To-Failure at 9.6V, 10.8V, 11.4V, 12.0V, and 12.6V for Tests Done at 105°C.

The methodology of this accelerated testing is as follows: (1) multiple failure distributions are generated at various combinations of voltage and temperature (usually above rated values), (2) the degree of acceleration caused by changes in voltage and absolute temperature (observed separately) is quantified as the ratio of the median lifetimes, and (3) values of *n* and *Ea* are determined so as to best fit the acceleration equation to the experimental data. The objective of this accelerated testing is to predict the t_{50} of devices under normal, non-accelerated operating conditions by applying equation (2) with the derived values of *n* and *Ea* and the known median life under accelerated conditions.

Data collected at 105°C and five voltages appear in fig. 6. The similarity between the series is clear. Based on the well behaved nature of the data, it seems reasonable to project that further decreases in test voltage would produce failure distributions whose only difference would be longer median life.

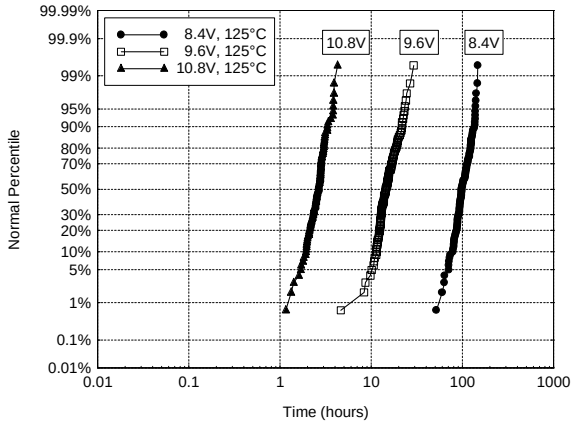

Fig. 7. Lognormal Plot of Failure Percentile versus Time-To-Failure at 8.4V, 9.6V, and 10.8V for Tests Done at 125°C.

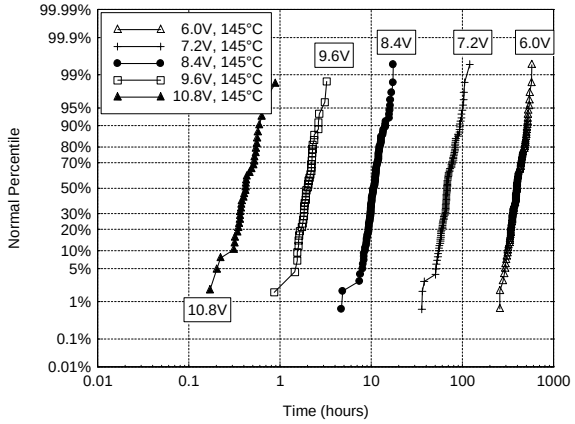

Fig. 8. Lognormal Plot of Failure Percentile versus Time-To-Failure at 6.0V, 7.2V, 8.4V, 9.6V, and 10.8V for Tests Done at 145°C.

Figs. 7 and 8 show additional data collected at constant temperatures in which the voltage was changed for each dataset. In each plot, the median time-to-failure for the groups changes proportionally to the test voltage. The uniformity of the shifts suggests predictable improvements from changes to

lower voltages as long as the percentage of the downward shifts is chosen consistently.

Fig. 9 is a plot of median life, t_{50}, versus test voltage at 85°C, 105°C, 125°C, 145°C, and 165°C. In this figure, each failure distribution discussed in figs. 6-8 is represented by its t_{50} point. These points are plotted on "log-log" scale to allow the time-ordered data points to fall into straight lines. Lines whose slope represents the voltage stress exponent from equation (2) can be estimated using these t_{50} points.

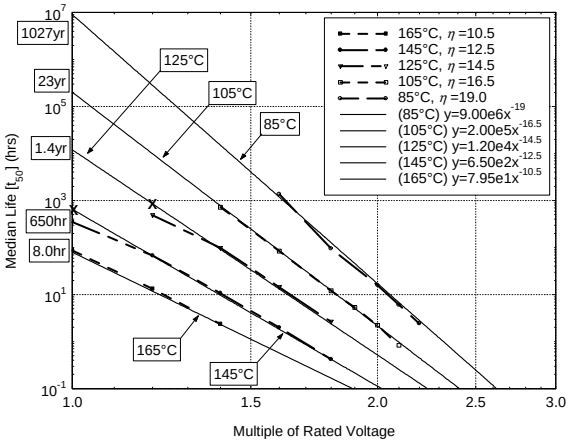

Fig. 9. Plot of Median Life versus Test Voltage at 85°C, 105°C, 125°C, 145°C, and 165°C on Log-Log Scale.

The values for the voltage stress exponent range from 10.5 to 19. This lack of consistency from group to group represents an interaction between test voltage and temperature not considered in the acceleration formula. Recall from figs. 2 and 3 that device temperature rises above the ambient test temperature due to internal heating. This heating results from high leakage current. The leakage, power dissipated, and the resulting temperature rise increase with rising test temperature and test voltage. Thus test temperature and test voltage are not truly independent stress factors since both act to increase the core temperature of the capacitor above the ambient test temperature, thus elevating the overall stress level. This interaction produces lower than expected life as temperature and voltage increase. Regardless, the median life data points for tests conducted at a constant temperature show consistent behavior which can be characterized and predicted.

The x-axis of fig. 9 extends down to rated voltage. This enables an estimate of life test performance at the maximum rated conditions for the parts. Following the line of 85°C results back to the rated voltage point, the fit line indicates these parts would reach their t_{50} after 1027 years at maximum rated conditions. Going further, if half-rated voltage is used, the t_{50} estimate stretches into the millions of years.

Notice that the t_{50} point at 1.2Vr in the 125°C data does not fall on the line for that distribution. Likewise, the t_{50} point at 1.0Vr in the 145°C data falls short of predictions based on data for that temperature taken at other voltages. A follow-up investigation into this discrepancy has revealed the mounting conditions for these two sample groups to be slightly different from the rest of the test groups. Subsequent testing of capacitors from a related batch has shown that results for these conditions should have fallen closer to the values predicted by the tests done at the same temperature, but higher voltages. The correct position for the 125°C and 145°C data points are approximately 850 hours and 690 hours respectively (marked by X's on the graph).

We might also be curious about the expected time until the onset of wearout at maximum rated conditions in addition to median life. Judging from figs 6-8, the bulk of the failure distributions shown generally occupy less than a decade of time. Bearing this in mind, a safe estimate for the onset of wearout is one-half decade prior to the projected median life (roughly a factor of 3). So, a conservative estimate for the onset of failures would be $t_{50}/3$. For these capacitors at maximum rated conditions, we can expect to start seeing failures after 342 years of use.

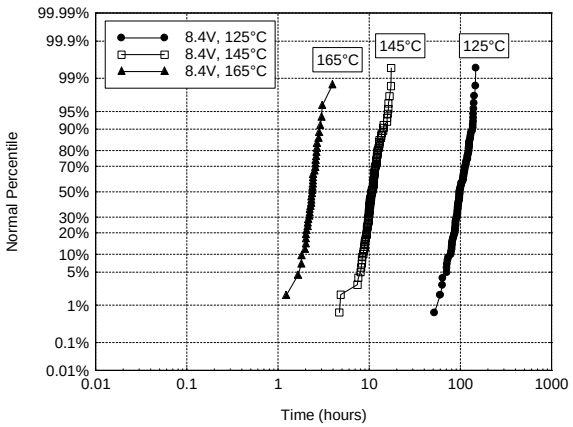

Fig. 10. Lognormal Plot of Failure Percentile versus Time-To-Failure at 125°C, 145°C, and 165°C for Tests Done at 8.4V.

The next three figures will focus on temperature acceleration rather than voltage acceleration. The

same time-to-failure information will be used, but the data will be grouped by voltage rather than temperature. The goal is to calculate the activation energy for equation (2). Figure 10 shows all time-to-failure data collected at 8.4V (1.4 times rated voltage) with each data series representing a different temperature.

Figs. 11 and 12 contain data collected at 9.6V and 10.8V, respectively. Again, it is clear to see that all the distributions are similar as the temperature is changed from 85°C to 145°C. Given the consistent nature of the data, it seems reasonable to project that further decreases in temperature would produce failure distributions with longer median life.

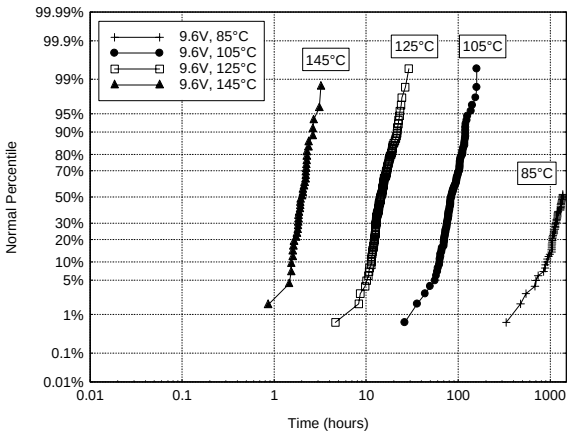

Fig. 11. Lognormal Plot of Failure Percentile versus Time-To-Failure at 105°C, 125°C, and 145°C for Tests Done at 9.6V.

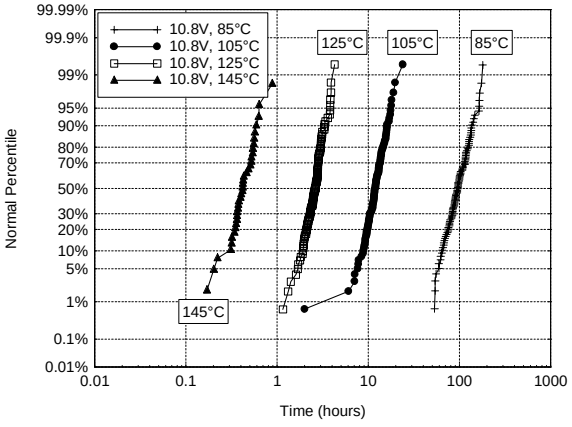

Fig. 12. Lognormal Plot of Failure Percentile versus Time-To-Failure at 85°C, 105°C, 125°C, and 145°C for Tests Done at 10.8V.

Fig. 13 is a plot of median life versus inverse absolute temperature at 1.0Vr, 1.2Vr, 1.4Vr, 1.6Vr, 1.8Vr, 1.9Vr, 2.0Vr, 2.1Vr, and 2.2Vr. As in fig. 9, each failure distribution discussed in figs. 10-12 has been reduced to a single statistic, t_{50}. The t_{50} points are plotted on a "semi-log" scale to linearize the Arrhenius temperature factor in equation (2). Nine lines have been fitted to the data points. Since there is only one data point for the 1.9Vr and 2.2Vr tests, these lines borrow their slope from adjacent datasets. Given the similar slope of the lines, this assumption seems reasonable. Equations for all the lines in fig. 13 appear in table I.

Table I
ACTIVATION ENERGY AND LINE EQUATIONS FOR TEMPERATURE ACCELERATION

Test Bias	Act. Energy	Fit Line
1.0Vr	*Ea* = 1.75eV	y = 16.5*exp[(1.75/8.63)*(x-2.2)*100]
1.2Vr	*Ea* = 1.55eV	y = 3.0*exp[(1.55/8.63)*(x-2.2)*100]
1.4Vr	*Ea* = 1.40eV	y = 0.6*exp[(1.40/8.63)*(x-2.2)*100]
1.6Vr	*Ea* = 1.25eV	y = 0.14*exp[(1.25/8.63)*(x-2.2)*100]
1.8Vr	*Ea* = 1.25eV	y = 0.0225*exp[(1.25/8.63)*(x-2.2)*100]
1.9Vr	*Ea* = 1.25eV	y = 0.008*exp[(1.25/8.63)*(x-2.2)*100]
2.0Vr	*Ea* = 1.25eV	y = 0.00325*exp[(1.25/8.63)*(x-2.2)*100]
2.1Vr	*Ea* = 1.25eV	y = 0.00125*exp[(1.25/8.63)*(x-2.2)*100]
2.2Vr	*Ea* = 1.25eV	y = 0.00045*exp[(1.25/8.63)*(x-2.2)*100]

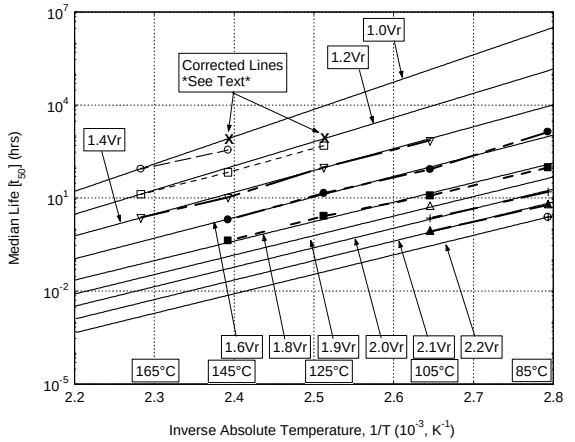

Fig. 13. Plot of Median Life versus Inverse Absolute Temperature at 1.0Vr, 1.2Vr, 1.4Vr, 1.6Vr, 1.8Vr, 1.9Vr, 2.0Vr, 2.1Vr, and 2.2Vr on Semi-Log Scale.

The lines for the 1.0Vr data and 1.2Vr data are based on only five points, two of which are already identified as erroneous. Although these points occur at 360 and 490 hours, predictions based on the more reliable data taken at higher test voltages at 125°C and 145°C (shown in figure 9) which are supported by results from independent tests performed on a related batch place the points at 690 and 850 hours. This changes the slope of the best-fit lines and the calculated activation energy for tests done at 1.0Vr and 1.2Vr.

Once corrections have been made to the fit lines, the activation energy for the test groups ranges from 1.25eV to 1.75eV. Again, the voltage-temperature interaction, previously observed in the voltage acceleration investigation, has affected the results. While the activation energies are not consistent from one test voltage to another, the values at each voltage still enable reliability predictions at other temperatures while using that voltage. Based on the limited data at 1.0Vr presented here at temperatures far removed from 85°C, the projected t_{50} time for these parts at maximum conditions becomes just over 360 years. Based on this prediction, the first failures from the group may occur after 100 years of use. Again, this prediction is based on only two data points whose temperatures are far removed from 85°C. Thus it is not thought to be as reliable as the life prediction based on the 85°C line of figure 9. Nevertheless, onset of failures at 100 years would still be considered to be quite acceptable reliability.

Summary and Conclusions

Acceleration to the onset of wearout without activating new or unusual failure mechanisms has been demonstrated by exposing tantalum polymer capacitors to temperature and electric field stress in excess of their rated maximums. The time-to-failure distributions for these devices did not alter their shape even under relatively severe test conditions.

Plots of median life versus test voltage and temperature produce families of curves that are proportionately spaced and reasonably linear when appropriately scaled with respect to the Prokopowicz and Vaskas acceleration equation. Based on these observations, time-to-failure under more normal conditions can be predicted with confidence by applying the failure model and values for the voltage stress exponent and activation energy that are derived from accelerated testing of samples from the device population.

For the devices tested in this study, projected median life at maximum rated conditions was more than 300 hundred years. Onset of failures, considering the well-behaved nature of the failure distributions, was calculated to be at least 100 years of constant use at rated voltage and 85°C. These results indicate that properly constructed polymer tantalum capacitors possess sufficient reliability to successfully replace traditional MnO_2 tantalums in modern applications.

Reference

[1] T. Prokopowicz and A. Vaskas, “Research and Development, Intrinsic Reliability, Subminiature Ceramic Capacitors,” Final Report, ECOM-90705-F, 1969 NTIS AD-864068.

[2] J. Paulsen and E. Reed, “Highly Accelerated Lifetesting (HALT) of KEMET Base-Metal-Electrode (BME) Ceramic Chip Capacitors,” CARTS ’01 Proceedings of the 21st Capacitor and Resistor Technology Symposium, p. 265 (2001).

[3] F. Jenson, Electronic Component Reliability, John Wiley & Sons, West Sussex, England, 1995, pp.8-11.